Published in final edited form as:
Top Organomet Chem. 2011 January 1; 503: 129–156. doi:10.1007/978-3-642-17429-2_6.

Palladium(III) in Synthesis and Catalysis

David C. Powers and **Tobias Ritter***
Department of Chemistry and Chemical Biology, Harvard University, 12 Oxford Street, Cambridge, Massachusetts

Abstract

While the organometallic chemistry of Pd in its (0), (+II), and (+IV) oxidation states is well-established, organometallic Pd(III) chemistry remains widely unexplored. Few characterized Pd(III) complexes are known, which has inhibited detailed study of the organometallic chemistry of Pd(III). In this review, the potential roles of both mono- and dinuclear Pd(III) complexes in organometallic chemistry will be discussed. While not widely recognized, Pd in the (+III) oxidation state may play a significant role in a variety of known Pd-catalyzed reactions.

Keywords

Pd(III); C–H functionalization; metal-metal bonding; bimetallic redox chemistry

1 Introduction

Palladium is among the most widely used metals for catalysis in organic chemistry, and the fundamental organometallic chemistry of palladium in the (0), (+II), and (+IV) oxidation states has been well-studied [1]. Organometallic Pd(I) complexes, while relatively less common, have been employed as precatalysts in organic synthesis [2-4]. By comparison, the organometallic chemistry of Pd(III) remains in its infancy. Few authentic Pd(III) complexes are known and the potential role of Pd(III) in catalysis is only now beginning to be elucidated. Herein, we will review the organometallic chemistry of Pd(III) and discuss the relevance of Pd(III) intermediates to Pd-catalyzed processes. We will review the organometallic chemistry of well-defined, isolated Pd(III) complexes, as well as organometallic chemistry in which the potential role of Pd(III) intermediates is currently more speculative. Based on the reports discussed herein, Pd(III) may be much more prevalent in Pd-catalyzed processes than has generally been recognized.

2 Mononuclear Pd(III) Chemistry

2.1 Mononuclear Pd(III) Werner-type Complexes

Palladium(II) has a d^8 electronic configuration and mononuclear Pd(II) complexes are generally square planar (Figure 1) [5]. Metal-based oxidation of mononuclear Pd(II) complexes by one-electron should result in paramagnetic, low-spin d^7, tetragonally distorted octahedral Pd(III) complexes [6]. Further one-electron oxidation should afford octahedral d^6 Pd(IV) complexes [5].

Unlike complexes based on Pt(III) [7-15], compounds containing Pd(III) are rare. A compound with the empirical formula PdF_3 was originally proposed to contain Pd(III)

*ritter@chemistry.harvard.edu .

[16,17], but was subsequently shown to by more appropriately formulated as $Pd^{2+}[PdF_6]^{2-}$ and contain Pd(II) and Pd(IV) [18,19]. The polyatomic anions PdF_4^- and PdF_6^{3-} have been prepared by solid-state synthesis [20-22]. Mononuclear coordination complexes containing Pd(III) have been observed by electrochemical measurements as well as EPR spectroscopy [23-30], although assignment of these complexes as containing Pd(III), and not Pd(II) with a singly oxidized ligand framework, has been the source of continuing discussion [31-34]. In 2010, the (+III) oxidation state of Pd was stabilized in a mixed Ni/Pd oligomeric M–X–M–X chain of the formulation $[Ni_{1-x}Pd_x(chxn)Br]Br_2$ (chxn = (1*R*,2*R*)-cyclohexanediamine) by electrochemical oxidation of a mixture of $[Ni(chxn)_2]Br_2$ and $[Pd(chxn)_2]Br_2$ [35,36].

Two mononuclear, Werner-type complexes based on Pd(III) have been characterized by X-ray crystallography. The X-ray crystal structure of mononuclear Pd(III) complex **1**, in which the Pd(III) center is supported by two 1,4,7-trithiacyclononane ligands, was reported in 1987 (Figure 2) [37-39]. An analogous complex (**2**), supported by 1,4,7-triazacyclononane ligands, was reported a year later [40]. Both complexes contain distorted octahedral Pd centers, as expected for low-spin, d^7 Pd(III) [6]. Detailed examination of the electrochemical and spectroscopic properties of Pd(III) complexes supported by macrocyclic polydentate ligands has indicated that the unpaired electron in **1** and **2** resides predominantly in the 4 d_z^2 orbital [41-46].

2.2 Mononuclear Pd(III) Complexes in Catalysis

Pd(III) in Pd-catalyzed Oxidative C–H Coupling Reactions—Palladium is a versatile transition metal for the catalysis of various carbon–carbon and carbon–heteroatom cross-coupling reactions [1]. Traditional C–C cross-coupling reactions employ pre-functionalized substrates – typically containing C–X (X = Cl, Br, I, OTf) and C–M (M = B, Sn, Zn, Mg) bonds respectively – and are generally accepted to proceed through Pd(0)/Pd(II) catalysis cycles [47]. Direct oxidative coupling of arene C–H bonds has the potential to generate the products of traditional cross-coupling chemistry without the need for pre-functionalized reaction partners (Figure 3a) [48-53]. A general catalysis cycle for such an oxidative coupling of aryl C–H bonds is outlined in Figure 3b. Initial C–H palladation at Pd(II) (**3**) would generate an aryl Pd(II) complex (**4**). Subsequently, a second C–H palladation could afford a heteroleptic biaryl Pd(II) complex (**5**), poised to undergo C–C bond-forming reductive elimination. The catalysis cycle is closed by re-oxidation of the thus formed Pd(0) (**6**) to Pd(II) (**3**) by an external oxidant. While biaryl Pd(II) intermediate **5** is typically proposed to undergo direct C–C reductive elimination, in the presence of an external oxidant, **5** could potentially be oxidized to a higher-valent species prior to the C–C bond forming event [54,55].

Single electron oxidation of biaryl Pd(II) complexes to afford Pd(III) species was observed during the electrochemical oxidation of *bis*-mesityl Pd(II) complex **7** (Figure 4) [56]. Complex **7**, which can be viewed as a model for oxidative C–H coupling intermediate **5** (Figure 3), undergoes a one-electron oxidation at 0.57 V, assigned to the Pd(II)/Pd(III) redox couple.

Oxidative C–H coupling reactions are frequently carried out in the presence of Ag(I) additives [57-64]. As described below, due to: 1) the demonstrated availability of one-electron oxidation processes for compounds such as **7** [56], 2) the propensity of Ag(I) to facilitate one-electron oxidative cleavage of Pd–C bonds [65] (*vide infra*), and 3) the frequency with which Ag(I) additives are employed in Pd-catalyzed cross-coupling chemistry [57-64], the reaction chemistry of Ag(I) salts with organometallic Pd(II) complexes has received experimental scrutiny.

In 2001, Milstein studied the reactivity of Pd(II) aryl complex **8** with one-electron oxidants galvinoxyl radical and AgOTf (Figure 5) [66]. Treatment of Pd(II) aryl complex **8** with AgOTf resulted in the formation of biphenyl along with Pd(II) triflate **10**. Similar reactivity was observed upon treatment of **8** with galvinoxyl radical. Milstein proposed that this oxidant-induced reductive coupling of aryl ligands proceeds through Pd(III) intermediate **9**. The authors speculated that Pd(III) aryl intermediate **9** may be better formulated as a Pd(II) complex with a pendant aryl radical ligand, generated by inner-sphere ligand-to-metal electron transfer. No organic product resulting from coupling of free organic radicals with solvent were observed, suggesting that biphenyl is not produced by radical combination of phenyl radicals generated by Pd–C bond homolysis. This observation led to the suggestion that intermediate **9** may be an aryl-bridged dinuclear complex, which can liberate biphenyl without the intermediacy of free radical chemistry [67].

The oxidatively induced reductive coupling of methyl ligands to afford ethane from Pd(II) dimethyl complex **11** was reported in 2009 by Mayer and Sanford [68]. Treatment of dimethyl Pd(II) complex **11** with ferrocenium hexafluorophosphate ($[Cp_2Fe]PF_6$; Fc^+), an outer-sphere, single-electron oxidant, led to the formation of ethane along with cationic Pd(II) complex 13 (Figure 6). Based on the electrochemical study of closely related *bis*-mesityl Pd(II) complex **7** (Figure 4) [56], the observed ethane formation was proposed to proceed via initial single-electron oxidation of **11** to Pd(III) complex **12**.

Three mechanisms for the formation of ethane from **12** were considered (Figure 7). In mechanism A, Pd(III) complex **12** undergoes Pd–C bond homolysis to afford Pd(II) complex **13** and methyl radicals, which subsequently combine to generate ethane. Similar Pd–C bond homolysis following single electron oxidation was proposed by Trogler during an independent study of the oxidation chemistry of Pd(II) methyl complexes with Fc^+ [65]. In mechanism B, direct reductive elimination from **12** affords ethane and mononuclear Pd(I) complex **14**, which further reacts with **11** and Fc^+ to generate Pd(II) complex **13**. Analogous chemistry has been proposed for coupling reactions from organonickel complexes [69-75]. In mechanism C, two equivalents of complex **12** undergo disproportionation to afford Pd(II) complex **13** and Pd(IV) intermediate **15**. Subsequent reductive elimination from **15** generates ethane and Pd(II) complex **13**. Similar disproportionation has been proposed from Pt(III) dimethyl complexes [76].

The observation that ethane formation is uninhibited by radical traps such as 1,4-cyclohexadiene and styrene suggests that ethane is not formed by combination of free methyl radicals and is inconsistent with free radical pathway A. To differentiate between pathways B and C, the oxidation of **11** with Fc^+ was carried out at low temperature in order to observe potential reaction intermediates. Treatment of **11** with Fc^+ at −80 °C led to the observation of Pd(II) complex **13** and Pd(IV) complex **15** (Figure 8). Subsequent warming to −30 °C led to the formation of ethane. Based on these observations, the authors concluded that pathway C is likely responsible for the formation of ethane in the reaction of **11** with Fc^+.

The chemistry of complex **11** with $AgPF_6$ was evaluated because Ag(I) is a common additive in Pd-catalyzed oxidative C–H coupling reactions [57-64] and a potential one-electron oxidant, similar to Fc^+. Treatment of dimethyl Pd(II) complex **11** with $AgPF_6$ resulted in the immediate formation of an intermediate (**16**), as observed by ^{1}H NMR spectroscopy, which subsequently generated **13**, ethane, and Ag mirror (Figure 9). The authors proposed that Ag(I) acts as an inner-sphere one-electron oxidant. Initial coordination of Ag(I) to Pd to generate **16**, followed by electron transfer, would furnish proposed Pd(III) intermediate **12**. Disproportionation of Pd(III) intermediate **12** to Pd(II) complex **13** and Pd(IV) intermediate **15** followed by reductive elimination from Pd(IV) complex **15**, as was

proposed in the oxidation of **11** with Fc^+, would then generate the observed reaction products.

Pd(III) in Pd-catalyzed Oxidative Carbon–Heteroatom Bond Forming Reactions—In 2009, two reports disclosed the use of single-electron oxidants in intramolecular Pd-catalyzed C–H amidation reactions. Yu and coworkers disclosed a Pd-catalyzed *N*-triflyl indoline (**18**) synthesis from *N*-triflyl phenethylamines (**17**) using single-electron oxidant $Ce(SO_4)_2$ (Figure 10) [77]. The authors proposed that this reaction proceeds through initial oxidation of Pd(II) to Pd(III). Glorius and coworkers reported a Pd-catalyzed *N*-acyl indoline (**20**) synthesis from *N*-acyl anilines (**19**) in the presence of AgOAc (Figure 11) [78]. While the authors favored a Pd(0)/Pd(II) catalysis cycle, they noted that the intermediacy of higher-valent Pd species could not be discounted given that AgOAc can serve as a single-electron oxidant.

Many questions remain to be addressed regarding the mechanisms of these amidation reactions. Primarily, are high-valent Pd intermediates involved, or are classical Pd(0)/Pd(II) catalysis cycles operative? If single-electron oxidation affords Pd(III) intermediates, does C–N bond formation proceed directly from Pd(III) or are Pd(IV) species, generated by either disproportionation of Pd(III) or further oxidation of Pd(III) to Pd(IV), the competent intermediates for C–N bond formation? Are potential high-valent intermediates mononuclear or is more than one palladium present during oxidation? Answers to these questions will provide insight into the potential role of high-valent Pd complexes in C–H amidation reactions.

Pd(III) in Kumada and Negishi Coupling Reactions—Knochel has noted remarkable rate accelerations for both Kumada [79] and Negishi [80] coupling reactions when performed in the presence of isopropyl iodide (Figure 12).

Oxidative addition of Pd(0) to isopropyl iodide has been shown to proceed via initial single electron transfer to generate transient Pd(I) intermediates and isopropyl radicals [81,82]. On the basis of a positive isopropyl iodide-induced radical-clock experiment (Figure 13), Knochel suggested that the observed rate acceleration in Kumada coupling reactions is due to the participation of a radical pathway and proposed a radical mechanism involving Pd(I) and Pd(III) radical chain carriers (Figure 14). The proposal of Pd(III) intermediates in Kumada coupling reactions is, to the best of our knowledge, the only proposal of Pd(III) intermediates under reducing conditions.

Pd(III) Intermediates in O_2 Insertion Reactions—Goldberg and coworkers proposed Pd(III) intermediates during an investigation of the reaction of dimethyl Pd(II) complex **24** with O_2 (Figure 15) [83].

Consistent with a radical chain mechanism, the rate of O_2 insertion was found to be sensitive to light, and the addition of radical initiator AIBN was required in order to observed reproducible reaction rates. Based on analysis of the kinetics of O_2 insertion into the Pd–C bond of **24**, a mechanism involving mononuclear Pd(III) intermediates was proposed (Figure 16). Palladium(III) intermediate **27**, formed by combination of dimethyl Pd(II) complex **24** with peroxy radical **26** [84], generates the observed Pd(II) peroxide **25** by homolytic Pd–C cleavage to reduce Pd(III) complex **27** and generate radical chain carrier Me·.

The mechanism of O_2 insertion into the Pd–C bond of **24** differs from the autoxidation of organic substrates due to the ability of Pd to attain high oxidation state intermediates. In hydrocarbon autoxidation, peroxy radical abstracts hydrogen without the intermediacy of

hypervalent intermediates. In the oxidation of **24**, the coordination number of Pd is proposed to increase from four to five upon reaction of Pd(II) complex **24** with peroxy radical (**26**).

2.3 Organometallic Chemistry of Isolated Pd(III) Complexes

The first example of organometallic chemistry from isolated, well-defined mononuclear Pd(III) complexes was reported by Mirica in 2010 [85]. Organometallic Pd(III) complexes **30** and **31** were prepared by controlled bulk-electrolysis of Pd(II) precursors **28** and **29**, respectively (Figure 17). Complex **33** was prepared by chemical oxidation of **32** with Fc^+. X-ray crystallographic analysis of **30**, **31**, and **33** revealed tetragonally distorted octahedral complexes, consistent with the expected Jahn-Teller distortion for mononuclear, low-spin Pd(III) complexes [6]. A combination of EPR spectroscopy and computational results suggests that the unpaired electron resides in the 4 d_{z^2} orbital, consistent with the MO description of octahedral Pd(III) in Figure 1.

Photolysis of **30** afforded a mixture of ethane, methane, and methyl chloride, along with Pd(II) complex **34** (Figure 18).

The addition of radical scavengers, such as TEMPO, suppressed the formation of ethane, methane, and methyl chloride, instead leading only to the observation of TEMPO-Me (**35**) and Pd(II) complex **34** (Figure 19). The observed reaction with radical scavengers is consistent with photo-induced homolytic Pd–C bond cleavage as the operative pathway for the formation of the observed organic products, although the observed organic products may also arise from radical combination of Me· with **30** to afford a transient Pd(IV) intermediate, which subsequently generates the observed products.

3 Dinuclear Pd(III) Chemistry

3.1 Dinuclear Pd(III) Complexes

Palladium(II) has a d^8 electronic configuration; the HOMO of mononuclear Pd(II) complexes is typically the d_{z^2} orbital (Figure 1) [5]. When two palladium nuclei are held in proximity such that electronic communication between the two metals is possible, mixing of the d-orbitals gives rise to the qualitative molecular orbital picture in Figure 20 [86]. Bonding antibonding interactions result from mixing of the d_{z^2}, d_{xy}, d_{xz} and d_{yz} orbitals; the $d_{x^2-y^2}$ is predominantly metal–ligand bonding and does not significantly participate in metal–metal bonding interactions.

Dinuclear Pd(II) Complexes—Both the metal-metal σ and σ* orbitals should be filled for dinuclear Pd(II) complexes (Figure 20). Based on these considerations alone, no attractive metal–metal interaction is expected; there is no Pd–Pd bond [87]. Second-order, symmetry-allowed mixing of the Pd d_{z^2} orbital with the 5p_z and the 5*s* orbital, however, perturbs the molecular orbital diagram based only on *d* orbital interactions [88-91]. In 2010, an evaluation of the bonding interactions between the Pd centers in acetate-bridged, dinuclear Pd(II) complex **36** was reported (Figure 21) [88]. Based on DFT calculations, the authors predicted a weak attractive interaction between the Pd centers in **36** and computed a Pd–Pd bond order of 0.11.

Pd(II)/Pd(III) Mixed Valence Complexes—Oxidation of dinuclear Pd(II) complexes by one electron is predicted to afford dinuclear Pd(II)/Pd(III) mixed valence complexes with a Pd–Pd bond order of 0.5 (Figure 20) [92]. Dinuclear Pd(II)/Pd(III) mixed valence complexes have been detected by EPR spectroscopy, although, similar to mononuclear systems, the unpaired electron is not always metal-centered [87,93]. Two examples of dinuclear Pd(II)/Pd(III) complexes bearing a metal-centered unpaired electron have been reported [94,95]. In

1988, Bear reported the EPR spectrum of tetra-bridged dinuclear complex **38**, prepared by electrochemical oxidation of **37** (Figure 22a) [95]. In 2007, Cotton reported the only crystallographically characterized mixed valence Pd(II)/Pd(III) complex (**40**; Figure 22b) [94]. Both **38** and **40** are paramagnetic and have EPR spectra consistent with a metal-based oxidation. The metal–metal distance in **40** is 0.052 Å shorter than the corresponding distance in Pd(II) complex **39**, consistent with a Pd–Pd bond order of 0.5.

Elegant electrochemical studies related to Bear's report of dinuclear Pd(II)/Pd(III) mixed valence complex **38** emphasize an important difference between the oxidation chemistry of mono- and dinuclear complexes. The electrochemistry of complex **38**, bearing four bridging ligands, and **41**, in which two ligands are bridging and two are chelating, was studied (Figure 23) [95]. Complex **41** displays oxidation behavior consistent with two electronically isolated Pd centers; a single two-electron oxidation wave was observed at 1.02 V. By contrast, complex **38** displays electrochemical behavior consistent with electronically coupled metal centers; a one-electron oxidation wave is observed at 0.65 V. Based on these electrochemical measurements, it was concluded that the electronic interaction between two palladium centers raises the HOMO energy by 370 mV and renders the dinuclear complex easier to oxidize than the complex with non-interacting metal centers. It is not clear why the Pd centers in **41** are electronically non-coupled, as many dinuclear Pd complexes bridged by two ligands display electrochemical behavior consistent with electronically coupled systems [92,96].

Dinuclear Pd(III) Complexes—Oxidation of dinuclear Pd(II) complexes by two electrons can result in dinuclear Pd(III) complexes with a metal–metal σ bond (Figure 20). Cotton reported the first dinuclear Pd(III) complex (**43**) in 1998 (Figure 24) [97]. Complex **43**, obtained by oxidation of dinuclear Pd(II) complex **42** with $PhICl_2$, is diamagnetic, consistent with the formation of a spin-paired Pd–Pd bond. Further, the metal–metal bond distance in **43** is 2.39 Å, a contraction of 0.16 Å as compared to Pd(II) complex **42** (Pd–Pd = 2.55 Å).

The first organometallic Pd(III) complexes (**44**–**46**) were reported in 2006 (Figure 25) [98]. Complexes **44**–**47** have been used as precatalysts for both the diborylation of terminal olefins and diborylation/cross-coupling tandem reactions (Figure 26) [99]. The role of the Pd(III) complexes in these reactions has not been established; the diborane reagents employed have been shown to immediately reduce the dinuclear Pd(III) complexes to Pd(II) species, and thus the Pd(III) complexes may be a precatalyst for lower-valent active catalysts.

3.2 Dinuclear Pd(III) Complexes in Catalysis

Pd-Catalyzed C–H Acetoxylation—Palladium-catalyzed aromatic C–H acetoxylation was first reported in 1966 [100,101]. In 1971, Henry proposed Pd(IV) intermediates in the Pd-catalyzed acetoxylation of benzene with $K_2Cr_2O_7$ in AcOH [102]. Subsequent reports by Stock [103] and Crabtree [104] also discussed the possible intermediacy of Pd(IV) complexes in the acetoxylation of benzene (Figure 27a). In 2004, Sanford reported the regioselective *ortho*-acetoxylation of 2-arylpyridines and proposed a reaction mechanism involving aromatic C–H metallation at Pd(II), oxidation of the resulting aryl Pd(II) intermediate to a Pd(IV) complex, and product-forming C–O reductive elimination (Figure 27b) [105-108].

In 2009, we suggested that Pd-catalyzed aromatic C–H acetoxylation may proceed via dinuclear Pd(III) complexes instead of via mononuclear Pd(IV) intermediates [109]. Based on dinuclear Pd(II) complex **36**, the product of cyclometallation of 2-phenylpyridine (**48**) with $Pd(OAc)_2$ [110], a synthesis cycle based on dinuclear Pd(III) complexes was

established (Figure 28). Oxidation of **36** with $PhI(OAc)_2$, a common oxidant in Pd-catalyzed aromatic acetoxylation, afforded dinuclear Pd(III) complex **50**. Complex **50** was observed to undergo C–O reductive elimination under pseudocatalytic conditions to generate **49** in 91% yield. The critical dinuclear Pd(III) intermediate (**50**) was crystallographically characterized; the Pd–Pd distance in **50** was measured to be 2.555 Å (compared with 2.872 Å for **36** [111]), consistent with the formation of a Pd–Pd single bond. Dinuclear Pd(III) complex **50** was found to be a kinetically competent catalyst in the acetoxylation of 2-phenylpyridine with $PhI(OAc)_2$.

Pd-Catalyzed C–H Chlorination—Fahey reported the Pd-catalyzed directed aromatic C–H chlorination of azobenzene using Cl_2 in 1970 (Figure 29) [112,113], and Sanford reported the Pd-catalyzed directed aromatic C–H chlorination of 2-arylpyridines with NCS in 2004 (chlorination reaction shown in Figure 30) [105, 114-116].

In 2010, we reported an investigation of the mechanism of the $Pd(OAc)_2$-catalyzed chlorination of benzo[*h*]quinoline (**51**) with NCS (*N*-chlorosuccinimide) (Figure 30) [96,117]. Elucidation of the salient features of the mechanism operative in catalysis was enabled by identification of the catalyst resting state, which was found to be succinate-bridged dinuclear Pd(II) complex **53**. The two palladium centers in **53** are held in proximity (Pd–Pd = 2.863 Å) by the bridging succinate ligands as established by x-ray crystallography.

Using resting state **53** as the catalyst for the chlorination reaction shown in Figure 30, the rate law of chlorination was determined to be: rate = k [**53**] [NCS] [AcO^-], which implies that oxidation is the turnover limiting step in catalysis. Further, the observed first-order dependence on dinuclear resting state **53** implies that two Pd centers participate in oxidation. The unexpected co-catalysis by acetate ions – generated by acetate for succinate exchange during formation of **53** – is consistent with a rate-determining transition state for oxidation in which acetate and NCS each interact with one of the Pd centers of resting state **53**, generating a dinuclear Pd(III) intermediate (Figure 31).

The experimentally derived rate law for chlorination is consistent with dinuclear Pd(III) complex **54** being the immediate product of oxidation during catalysis. Complex **54** has one apical chloride ligand and one apical acetate ligand and thus, upon thermolysis, could undergo either C–Cl reductive elimination, to generate **52**, or C–O reductive elimination, to generate **55** (Figure 32). We evaluated and confirmed the kinetic and chemical competence of **54** as an intermediate for chlorination. Chemoselective C–Cl reductive elimination from **54** was observed upon warming **54** above −78 °C (200 : 1 ratio of **52** to **55**). The observed ratio of **52** to **55** in the thermal decomposition of preformed **54** is consistent with the product distribution from the $Pd(OAc)_2$-catalyzed chlorination of benzo[*h*]quinoline (**51**). Using 10 mol% $Pd(OAc)_2$, a 200 : 1 ratio of **52** to **55** was observed (Figure 32).

Pd-Catalyzed C–H Arylation—Deprez and Sanford reported an investigation of the mechanism of $Pd(OAc)_2$-catalyzed arylation of 2-arylpyridine derivatives with diaryliodonium salt **57** in 2009 (Figure 33) [118]. The catalyst resting state was proposed to be mononuclear Pd complex **59**. By examining the initial rate of arylation as a function of [$Pd(OAc)_2$], the rate law of arylation was determined to be second order in Pd. In combination with the observation that oxidation is the turnover-limiting step in catalysis, the experimentally determined rate law is consistent with two Pd centers participating in oxidation during catalysis.

Sanford proposed the product of oxidation during catalysis to be one of the two constitutional isomers of a high-valent dinuclear Pd complex shown in Figure 34 and

suggested that the second palladium center in either **60** or **61** functions as an auxiliary ligand to the metal center that mediates the C–C bond formation.

3.3 Role of Dinuclear Core During Redox Chemistry

Carbon–heteroatom reductive elimination from dinuclear transition metal complexes, as was proposed by us [96,109] as the product-forming step in Pd-catalyzed C–H acetoxylation and chlorination reactions, is rare. The two formulations of the high-valent, dinuclear Pd intermediate in arylation proposed by Sanford (**60** and **61**) highlight that reductive elimination from dinuclear Pd structures could, in principle, proceed with either redox chemistry at both metals (bimetallic reductive elimination; reductive elimination from **60**) or with redox chemistry at a single metal (monometallic redox chemistry; reductive elimination from **61**). While structures **60** and **61** do not differ in composition, they do differ in their respective potentials for metal-metal redox cooperation to be involved in C–C bond forming reductive elimination.

In 2010, we reported a study regarding the role of the dinuclear core during C–Cl reductive elimination from **62**, an analog of the dinuclear Pd complexes that have been proposed in catalysis (Figure 35) [96,119]. Experimental results established that reductive elimination from **62** proceeds without fragmentation of the dinuclear core; C–Cl bond formation proceeds from a dinuclear complex.

To probe the role of the dinuclear core during reductive elimination (i.e. mono- versus bimetallic reductive elimination), the electron binding energies of each Pd center were computed as a function of reaction progress. The electron binding energy is a measure of the energy required to remove an electron from a particular orbital to infinite separation. The electron binding energy of an electron decreases during reduction and increases during oxidation. For metal centers with similar ligand environments, electron binding energy is well correlated with formal oxidation state [120-124].

The computed electron binding energies of Pd_a and Pd_b during the low energy reductive elimination pathway from **A**, the computed structure of **62**, monotonically decrease during reduction from Pd(III) (**A**) to Pd(II) (**D**). The observed trends are consistent with simultaneous redox chemistry at both metal centers during C–Cl reductive elimination (Figure 36).

For comparison, the electron binding energies of the palladium centers during a hypothetical pathway involving a Pd(II)/Pd(IV) mixed valence intermediate were also computed (Figure 37). For hypothetical reductive elimination via a Pd(II)/Pd(IV) mixed valence complex (**E**), the electron binding energies of Pd_a and Pd_b diverge during Pd(III)/Pd(III) to Pd(II)/Pd(IV) disproportionation (**A** → **E**). Subsequent reductive elimination is accompanied by a convergence of the electron binding energies as both Pd centers are becoming Pd(II) (**E** → **D**). That the electron binding energy profiles for the computed reductive elimination pathway (Figure 36) and hypothetical monometallic reductive elimination pathways (Figure 37) are different is consistent with the assertion of metal-metal redox synergy during reductive elimination from **62**.

In addition, the energetic barrier to reductive elimination from **62** has been calculated as a function of metal–metal bond length. As the metal-metal distance is increased, orbital overlap, which mediates redox communication during reductive elimination, is reduced. The barrier to reductive elimination is positively correlated with the metal-metal distance; as the metals are increasingly separated, reductive elimination becomes increasingly energetically demanding. These calculations suggest that metal-metal redox synergy, in which the redox

chemistry of reductive elimination is shared by two metals, lowers the energetic barrier to reductive elimination versus related processes involving a single metal.

Discussion of High-Valent Pd Intermediates Relevant in Pd-Catalyzed C–H Oxidations—From the seminal studies regarding the oxidation of benzene by Henry [102], Stock [103], and Crabtree [104], to the vast array of Pd-catalyzed aromatic C–H functionalizations reported in the last five years [125-128], Pd-catalyzed aromatic C–H oxidation continues to be an area of intense methodological and mechanistic investigation. Early mechanism proposals for the acetoxylation of aromatic C–H bonds invoked Pd(IV) intermediates. While mononuclear Pd(IV) complexes have been prepared and the intimate mechanisms of reductive elimination from these complexes have been elucidated [107,108,129-132], the relevance of Pd(IV) complexes to catalysis has not yet been established. Frequently, aromatic C–H palladation is the turnover-limiting step in Pd-catalyzed C–H oxidation reactions [109,133]. When palladation is turnover limiting, reaction kinetics analysis provides detailed information about the mechanism of metallation, not the mechanism of oxidation and cannot provide any information regarding the identity of potential high-valent intermediates.

Elucidation of the catalysis cycle that is operative during a given transformation requires direct investigation of the reaction during catalysis. Elucidation of the mechanism of oxidation relevant to catalysis by kinetics analysis requires a reaction in which oxidation is turnover limiting. In both the chlorination [96,117] and arylation [118] of 2-arylpyridine derivatives, oxidation is the turnover-limiting step of catalysis; in both reactions, kinetics analysis has revealed that two Pd centers are required for oxidation during catalysis. The structures of the proposed dinuclear Pd(III) complexes relevant to chlorination have been established by independent synthesis. A catalysis cycle, which is consistent with the results of all studies in which the identity of high-valent intermediates could be probed, is presented in Figure 38. Following C–H metallation, nucleophile-assisted bimetallic oxidation affords a dinuclear Pd(III) complex. Subsequent reductive elimination from this high-valent dinuclear complex affords the observed organic fragments and Pd(II). Although the results were obtained during study of the chlorination of benzo[*h*]quinoline, they may be relevant to a variety of other C–H oxidation reactions. While detailed experimentation regarding the specific mechanism of individual reactions remains to be examined, we suggest that a bimetallic redox mechanism based on dinuclear Pd(III) complexes is a viable conceptual framework for Pd-catalyzed aromatic C–H oxidation reactions.

4 Outlook

Herein, we have reviewed the organometallic chemistry of Pd(III), discussing examples of both well-defined Pd(III) complexes that participate in organometallic reactions, as well as examples in which the potential involvement of Pd(III) is more speculative at this time. We have discussed oxidative C–H coupling reactions in which biaryl Pd(II) intermediates may be diverted from the traditional Pd(0)/Pd(II) redox cycle in the presence of one-electron oxidants, allowing access to catalytically relevant mononuclear Pd(III) intermediates. We have also examined the recent proposal that many Pd-catalyzed oxidative C–H functionalization reactions may proceed via dinuclear Pd(III) complexes which undergo product-forming reductive elimination with redox participation of both metal centers. In both oxidative C–H coupling reactions as well as Pd-catalyzed C–H oxidations, Pd(III) intermediates have been discovered in reactions previously believed to proceed via more traditional two-electron, monometallic Pd redox cycles. Based on these proposals, Pd(III), in both mono- and dinuclear complexes, may play a much more prominent role in catalysis than has previously been appreciated. We anticipate that the unique reactivity of both mono-

and dinuclear Pd complexes will provide a foundation for the discovery of new reactions mediated by Pd(III) in the future.

Acknowledgments

We gratefully acknowledge financial support for this work from the NIH-NIGMS (GM088237).

References

1. Negishi, E., editor. Handbook of Organopalladium chemistry for Organic Synthesis. John Wiley & Sons, Inc.; New York: 2002.
2. Murahashi T, Kurosawa H. Coord Chem Rev. 2002; 231:207–228.
3. Markert C, Neuburger M, Kulicke K, Meuwly M, Pfaltz A. Angew Chem Int Ed. 2007; 46:5892–5895.
4. Hama T, Hartwig JF. Org Lett. 2008; 10:1545–1548. [PubMed: 18358038]
5. Albright TA. Tetrahedron. 1982; 38:1339–1388.
6. Miessler, GL.; Tarr, DA. Inorganic Chemistry. Pearson Education, Inc.; Upper Saddle River, New Jersey: 2004.
7. Canty AJ, Gardiner MG, Jones RC, Rodemann T, Sharma M. J Am Chem Soc. 2009; 131:7236–7237. [PubMed: 19422235]
8. Bonnington KJ, Jennings MC, Puddephatt RJ. Organometallics. 2008; 27:6521–6530.
9. Roundhill DM, Gray HB, Che CM. Acc Chem Res. 1989; 22:55–61.
10. Matsumoto K, Sakai K. Advances in Inorganic Chemistry. 2000; 49:375–427.
11. Lippert B. Coord Chem Rev. 1999; 182:263–295.
12. Zipp AP. Coord Chem Rev. 1988; 84:47–83.
13. Blake AJ, Gould RO, Holder AJ, Hyde TI, Lavery AJ, Odulate MO, Schröder M. J Chem Soc, Chem Commun. 1987:118–120.
14. Usón R, Forniés J, Tomás M, Menjón B, Sünkel K, Bau R. J Chem Soc, Chem Commun. 1984:751–752.
15. Usón R, Forniés J, Tomás M, Menjón B, Bau R, Sünkel K, Kuwabara E. Organometallics. 1986; 5:1576–1581.
16. Nyholm RS, Sharpe AG. J Chem Soc. 1952:3579–3587.
17. Sharpe AG. J Chem Soc. 1950:3444–3450.
18. Bartlett N, Rao PR. Proc Chem Soc London. 1964:393–394.
19. Tressaud A, Wintenberger M, Bartlett N, Hagenmuller P. C R Acad Sc Paris. 1976; 282:1069–1072.
20. Tressaud A, Khairoun S, Dance JM, Grannec J, Portier J, Hagenmuller P. J Fluorine Chem. 1982; 21:28.
21. Tressaud A, Khairoun S, Dance JM, Hagenmuller P. Z Anorg Allg Chem. 1984; 517:43–58.
22. Tressaud A, Khairoun S, Grannec J, Dance JM, Hagenmuller P. J Fluorine Chem. 1985; 29:39.
23. Jasper SA, Huffman JC, Todd LJ. Inorg Chem. 1998; 37:6060–6064. [PubMed: 11670743]
24. Eachus RS, Graves RE. J Chem Phys. 1976; 65:5445–5452.
25. Krigas T, Rogers MT. J Chem Phys. 1971; 54:4769–4775.
26. Raizman A, Barak J, Suss JT. Phys Rev B. 1985; 31:5716–5721.
27. Lane GA, Geiger WE, Connelly NG. J Am Chem Soc. 1987; 109:402–407.
28. Möller E, Kirmse R. Inorg Chim Acta. 1997; 257:273–276.
29. Luca V, Kukkadapu R, Kevan L. J Chem Soc, Faraday Trans. 1991; 87:3083–3089.
30. Warren LF, Hawthorn MF. J Am Chem Soc. 1968; 90:4823–4828.
31. Kirmse R, Stach J, Dietzsch W, Steimecke G, Hoyer E. Inorg Chem. 1980; 19:2679–2685.
32. Pandey KK. Coord Chem Rev. 1992; 121:1–42.

33. Ray K, Weyhermüller T, Neese F, Wieghardt K. Inorg Chem. 2005; 44:5345–5360. [PubMed: 16022533]
34. Motoyama T, Shimazaki Y, Yajima T, Nakabayashi Y, Naruta Y, Yamauchi O. J Am Chem Soc. 2004; 126:7378–7385. [PubMed: 15186177]
35. Yamashita M, Takaishi S. Chem Commun. 2010; 46:4438–4448.
36. Takaishi S, Wu H, Xie J, Kajiwara T, Breedlove BK, Miyasaka H, Yamashita M. Inorg Chem. 2010; 49:3694–3696. [PubMed: 20230015]
37. Blake AJ, Holder AJ, Hyde TI, Schröder M. J Chem Soc, Chem Commun. 1987:987–988.
38. Blake AJ, Holder AJ, Hyde TI, Roberts YV, Lavery AJ, Schröder M. J Organomet Chem. 1987; 323:261–270.
39. Matsumoto M, Itoh M, Funahashi S, Takagi HD. Can J Chem. 1999; 77:1638–1647.
40. Blake AJ, Gordon LM, Holder AJ, Hyde TI, Reid G, Schröder M. J Chem Soc, Chem Commun. 1988:1452–1454.
41. McAuley A, Whitcombe TW. Inorg Chem. 1988; 27:3090–3099.
42. Hunter G, McAuley A, Whitcombe TW. Inorg Chem. 1988; 27:2634–2639.
43. Reid G, Blake AJ, Hyde TI, Schröder M. J Chem Soc, Chem Commun. 1988:1397–1399.
44. Blake AJ, Reid G, Schröder M. J Chem Soc, Dalton Trans. 1990:3363–3373.
45. Blake AJ, Crofts RD, de Groot B, Schröder M. J Chem Soc, Dalton Trans. 1993:485–486.
46. Reid G, Schröder M. Chem Soc Rev. 1990; 19:239–269.
47. Hartwig, JF. Organotransition Metal Chemistry. University Science Books; Sausalito, California: 2010.
48. Ackermann L, Vicente R, Kapdi AR. Angew Chem Int Ed. 2009; 48:9792–9826.
49. Alberico D, Scott ME, Lautens M. Chem Rev. 2007; 107:174–238. [PubMed: 17212475]
50. Campeau LC, Fagnou K. Chem Commun. 2006:1253–1264.
51. McGlacken GP, Bateman LM. Chem Soc Rev. 2009; 38:2447–2464. [PubMed: 19623360]
52. Pascual S, de Mendoza P, Echavarren AM. Org Biomol Chem. 2007; 5:2727–2734. [PubMed: 17700837]
53. Stuart DR, Fagnou K. Science. 2007; 316:1172–1175. [PubMed: 17525334]
54. Kalyani D, Sanford MS. J Am Chem Soc. 2008; 130:2150–2151. [PubMed: 18229926]
55. Kalyani D, Satterfield AD, Sanford MS. J Am Chem Soc. 2010; 132:8419–8427. [PubMed: 20515033]
56. Klein A, Niemeyer M. Z Anorg Allg Chem. 2000; 626:1191–1195.
57. Chen X, Goodhue CE, Yu JQ. J Am Chem Soc. 2006; 128:12634–12635. [PubMed: 17002342]
58. Cho SH, Hwang SJ, Chang S. J Am Chem Soc. 2008; 130:9254–9256. [PubMed: 18582040]
59. Stuart DR, Villemure E, Fagnou K. J Am Chem Soc. 2007; 129:12072–12073. [PubMed: 17880083]
60. Takahashi M, Masui K, Sekiguchi H, Kobayashi N, Mori A, Funahashi M, Tamaoki N. J Am Chem Soc. 2006; 128:10930–10933. [PubMed: 16910689]
61. Potavathri S, Dumas AS, Dwight TA, Naumiec GR, Hammann JM, DeBoef B. Tetrahedron Lett. 2008; 49:4050–4053. [PubMed: 19652690]
62. Campeau LC, Parisien M, Jean A, Fagnou K. J Am Chem Soc. 2006; 128:581–590. [PubMed: 16402846]
63. Lebrasseur N, Larrosa I. J Am Chem Soc. 2008; 130:2926–2927. [PubMed: 18278918]
64. René O, Fagnou K. Org Lett. 2010; 12:2116–2119. [PubMed: 20380389]
65. Seligson AL, Trogler WC. J Am Chem Soc. 1992; 114:7085–7089.
66. Kraatz HB, van der Boom ME, Ben-David Y, Milstein D. Isr J Chem. 2001; 41:163–171.
67. Ozawa F, Fujimori M, Yamamoto T, Yamamoto A. Organometallics. 1986; 5:2144–2149.
68. Lanci MP, Remy MS, Kaminsky W, Mayer JM, Sanford MS. J Am Chem Soc. 2009; 131:15618–15620. [PubMed: 19824643]
69. Coronas JM, Muller G, Rocamora M. J Organomet Chem. 1986; 301:227–236.
70. Ceder RM, Granell J, Muller G, Font-Bardía M, Solans X. Organometallics. 1996; 15:4618–4624.

71. Higgs AT, Zinn PJ, Simmons SJ, Sanford MS. Organometallics. 2009; 28:6142–6144.
72. Tsou TT, Kochi JK. J Am Chem Soc. 1979; 101:7547–7560.
73. Matsunaga PT, Hillhouse GL, Rheingold AL. J Am Chem Soc. 1993; 115:2075–2077.
74. Koo K, Hillhouse GL. Organometallics. 1995; 14:4421–4423.
75. Higgs, AT.; Zinn, PJ.; Sanford, MS. Organometallics asap. 2010.
76. Johansson L, Ryan OB, Rømming C, Tilset M. Organometallics. 1998; 17:3957–3966.
77. Mei TS, Wang X, Yu JQ. J Am Chem Soc. 2009; 131:10806–10807. [PubMed: 19606861]
78. Neumann JJ, Rakshit S, Dröge T, Glorius F. Angew Chem Int Ed. 2009; 48:6892–6895.
79. Manolikakes G, Knochel P. Angew Chem Int Ed. 2009; 48:205–209.
80. Kienle M, Knochel P. Org Lett. 2010; 12:2702–2705. [PubMed: 20481437]
81. Kramer AV, Labinger JA, Bradley JS, Osborn JA. J Am Chem Soc. 1974; 96:7145–7147.
82. Kramer AV, Osborn JA. J Am Chem Soc. 1974; 96:7832–7833.
83. Boisvert L, Denney MC, Hanson SK, Goldberg KI. J Am Chem Soc. 2009; 131:15802–15814. [PubMed: 19827779]
84. Kamaraj K, Bandyopadhyay D. Organometallics. 1999; 18:438–446.
85. Khusnutdinova JR, Rath NP, Mirica LM. J Am Chem Soc. 2010; 132:7303–7305. [PubMed: 20462195]
86. Cotton, FA.; Murillo, CA.; Walton, RA., editors. Multiple Bonds Between Metal Atoms. Springer Science and Business Media, Inc.; New York: 2005.
87. Cotton FA, Matusz M, Poli R, Feng X. J Am Chem Soc. 1988; 110:1144–1154.
88. Bercaw JE, Durrell AC, Gray HB, Green JC, Hazari N, Labinger JA, Winkler JR. Inorg Chem. 2010; 49:1801–1810. [PubMed: 20092286]
89. Xia BH, Che CM, Zhou ZY. Chem-Eur J. 2003; 9:3055–3064.
90. Pan QJ, Zhang HX, Zhou X, Fu HG, Yu HT. J Phys Chem A. 2007; 111:287–294. [PubMed: 17214466]
91. Yip HK, Lai TF, Che CM. J Chem Soc, Dalton Trans. 1991:1639–1641.
92. Berry JF, Cotton FA, Ibragimov SA, Murillo CA, Wang X. Inorg Chem. 2005; 44:6129–6137. [PubMed: 16097835]
93. Cotton FA, Matusz M, Poli R. Inorg Chem. 1987; 26:1472–1474.
94. Berry JF, Bill E, Bothe E, Cotton FA, Dalal NS, Ibragimov SA, Kaur N, Liu CY, Murillo CA, Nellutla S, North JM, Villagrán D. J Am Chem Soc. 2007; 129:1393–1401. [PubMed: 17263424]
95. Yao CL, He LP, Korp JD, Bear JL. Inorg Chem. 1988; 27:4389–4395.
96. Powers DC, Ritter T. Nat Chem. 2009; 1:302–309.
97. Cotton FA, Gu J, Murillo CA, Timmons DJ. J Am Chem Soc. 1998; 120:13280–13281.
98. Cotton FA, Koshevoy IO, Lahuerta P, Murillo CA, Sanaú M, Ubeda MA, Zhao Q. J Am Chem Soc. 2006; 128:13674–13675. [PubMed: 17044680]
99. Penno D, Lillo V, Koshevoy IO, Sanaú M, Ubeda MA, Lahuerta P, Fernández E. Chem Eur J. 2008; 14:10648–10655.
100. Davidson JM, Triggs C. Chem Ind (London). 1966:457.
101. Tisue T, Downs WJ. J Chem Soc D. 1969:410a.
102. Henry PM. J Org Chem. 1971; 36:1886–1890.
103. Stock LM, Tse K, Vorvick LJ, Walstrum SA. J Org Chem. 1981; 46:1757–1759.
104. Yoneyama T, Crabtree RH. J Mol Catal A: Chem. 1996; 108:35–40.
105. Dick AR, Hull KL, Sanford MS. J Am Chem Soc. 2004; 126:2300–2301. [PubMed: 14982422]
106. Desai LV, Hull KL, Sanford MS. J Am Chem Soc. 2004; 126:9542–9543. [PubMed: 15291549]
107. Dick AR, Kampf JW, Sanford MS. J Am Chem Soc. 2005; 127:12790–12791. [PubMed: 16159259]
108. Racowski JM, Dick AR, Sanford MS. J Am Chem Soc. 2009; 131:10974–10983. [PubMed: 19459631]

109. Powers DC, Geibel MAL, Klein JEMN, Ritter T. J Am Chem Soc. 2009; 131:17050–17051. [PubMed: 19899740]
110. Gutierrez MA, Newkome GR, Selbin J. J Organomet Chem. 1980; 202:341–350.
111. Dinçer M, Özdemir N, Günay ME, Çetinkaya B. Acta Crystallogr, Sect E: Struct Rep Online. 2008; 64:M381.
112. Fahey DR. J Chem Soc D. 1970:417.
113. Fahey DR. J Organomet Chem. 1971; 27:283–292.
114. Whitfield SR, Sanford MS. J Am Chem Soc. 2007; 129:15142–15143. [PubMed: 18004863]
115. Kalyani D, Dick AR, Anani WQ, Sanford MS. Org Lett. 2006; 8:2523–2526. [PubMed: 16737304]
116. Kalyani D, Dick AR, Anani WQ, Sanford MS. Tetrahedron. 2006; 62:11483–11498.
117. Powers DC, Xiao DY, Geibel MAL, Ritter T. J Am Chem Soc. 2010; 132 in press.
118. Deprez NR, Sanford MS. J Am Chem Soc. 2009; 131:11234–11241. [PubMed: 19621899]
119. Powers DC, Benitez D, Tkatchouk E, Goddard WA, Ritter T. J Am Chem Soc. 2010; 132 asap.
120. Riggs WM. Anal Chem. 1972; 44:830–832.
121. Leigh GJ. Inorg Chim Acta. 1975; 14:L35–L36.
122. Chatt J, Elson CM, Hooper NE, Leigh GJ. J Chem Soc, Dalton Trans. 1975:2392–2401.
123. Cisar A, Corbett JD, Daake RL. Inorg Chem. 1979; 18:836–843.
124. Corbett JD. Inorg Chem. 1983; 22:2669–2672.
125. Lyons TW, Sanford MS. Chem Rev. 2010; 110:1147–1169. [PubMed: 20078038]
126. Xu L-M, Li B-J, Yang Z, Shi Z-J. Chem Soc Rev. 2010:712–733. [PubMed: 20111789]
127. Muñiz K. Angew Chem Int Ed. 2009; 48:9412–9423.
128. Chen X, Engle KM, Wang DH, Yu JQ. Angew Chem Int Ed. 2009; 48:5094–5115.
129. Canty AJ. Acc Chem Res. 1992; 25:83–90.
130. Byers PK, Canty AJ, Crespo M, Puddephatt RJ, Scott JD. Organometallics. 1988; 7:1363–1367.
131. Fu Y, Li Z, Liang S, Guo QX, Liu L. Organometallics. 2008; 27:3736–3742.
132. Furuya T, Benitez D, Tkatchouk E, Strom AE, Tang P, Goddard WA, Ritter T. J Am Chem Soc. 2010; 132:3793–3807. [PubMed: 20196595]
133. Stowers KJ, Sanford MS. Org Lett. 2009; 11:4584–4587. [PubMed: 19754074]

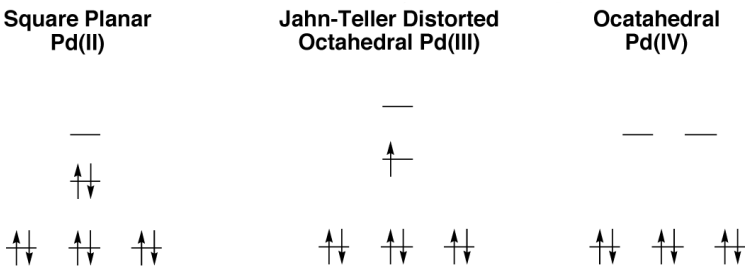

Fig. 1.
Electronic structure of mononuclear Pd(II), Pd(III), and Pd(IV)

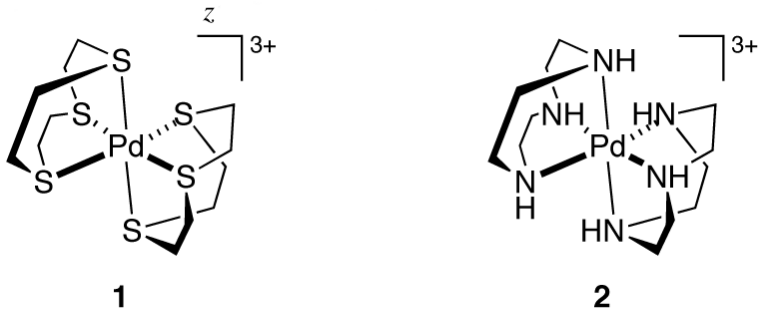

Fig. 2.
Crystallographically characterized examples of mononuclear Pd(III) Werner-type complexes

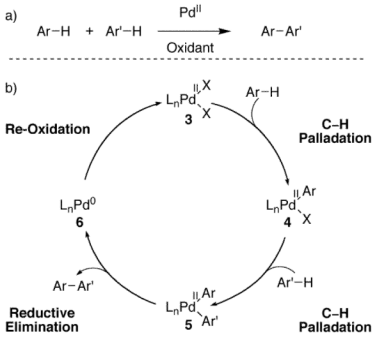

Fig. 3.
Generic Pd(0)/Pd(II) catalysis cycle for oxidative C–H cross-coupling

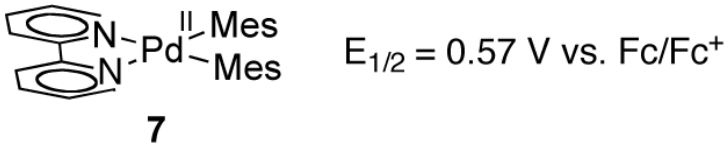

7

Fig. 4.

Bis-mesityl Pd(II) complex **7**, an analog of intermediate **5**, shows a reversible one-electron oxidation wave for the Pd(II)/Pd(III) couple at 0.57 V

Fig. 5.
Treatment of Pd(II) complex **8** with AgOTf generates Pd(II) complex **10** and biphenyl

Fig. 6.

Treatment of Pd(II) complex **11** with $[Cp_2Fe]PF_6$ (Fc^+) affords ethane and **13**

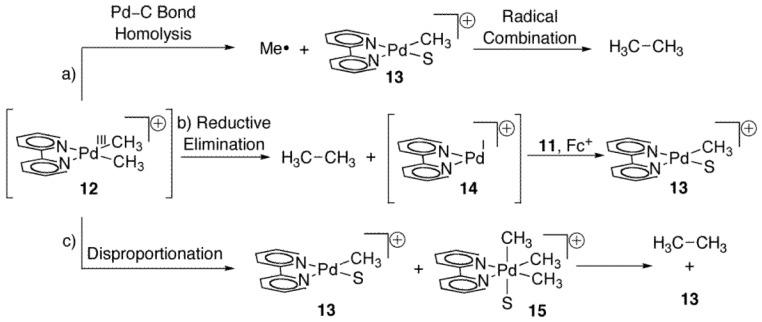

Fig. 7.
Mechanisms considered for the formation of ethane from Pd(III) complex **12**

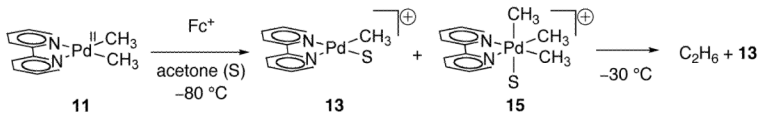

Fig. 8.

Pd(II) complex **13** and Pd(IV) complex **15** were observed following oxidation of **11** with Fc^+ at −80 °C

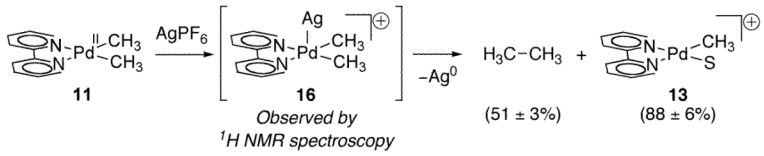

Fig. 9.

Treatment of **11** with $AgPF_6$ results in the formation of an intermediate, assigned as **16**, which subsequently generates ethane and **13**

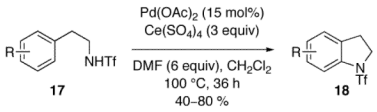

Fig. 10.
Pd-catalyzed C–H amidation reported by Yu

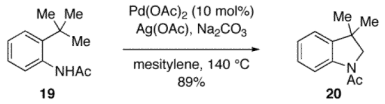

Fig. 11.
Pd-catalyzed C–H amidation reported by Glorius

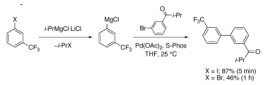

Fig. 12.
Isopropyl iodide catalyzed Kumada coupling reported by Knochel

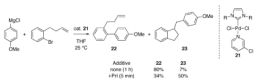

Fig. 13.
Observation of isopropyl iodide-induced radical clock (R = 2,6-di-*i*-Pr-C_6H_3)

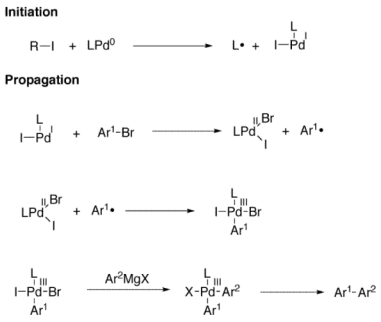

Fig. 14.
Mechanism proposed to account for the rate acceleration of cross-coupling observed in the presence of radical promoters

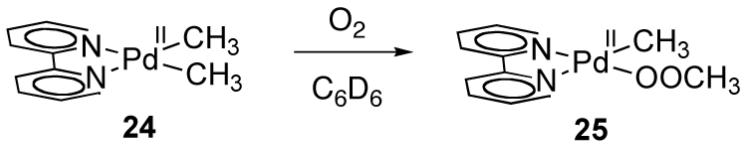

24 25

Fig. 15.
Pd(II) peroxide **25** is obtained by insertion of O_2 into the Pd–C bond of **24**

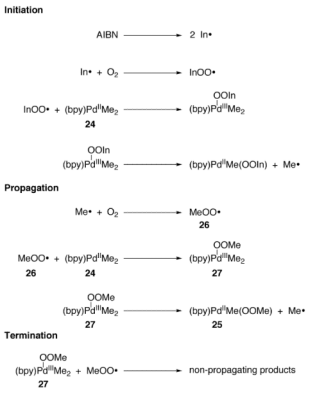

Fig. 16.
Proposed mechanism for the insertion of O_2 into the Pd–C bond of **24**

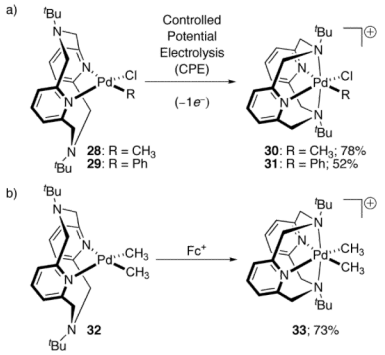

Fig. 17.

Mononuclear Pd(III) complexes **30** and **31** were prepared by Controlled Potential Electrolysis (CPE) of **28** and **29**, respectively. Complex **33** was prepared by oxidation of **32** with Fc^+

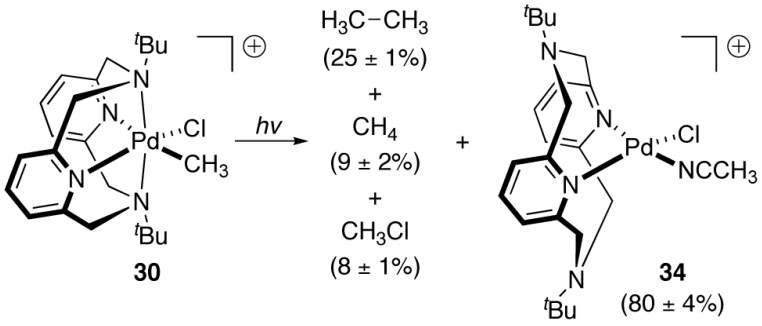

Fig. 18.

Photolysis of Pd(III) complex **30** generated ethane, methane, methyl chloride, and Pd(II) complex **34**

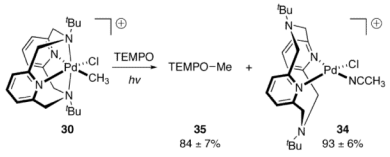

Fig. 19.

Photolysis in the presence of radical scavenger TEMPO suppressed formation of ethane, methane, and methyl chloride

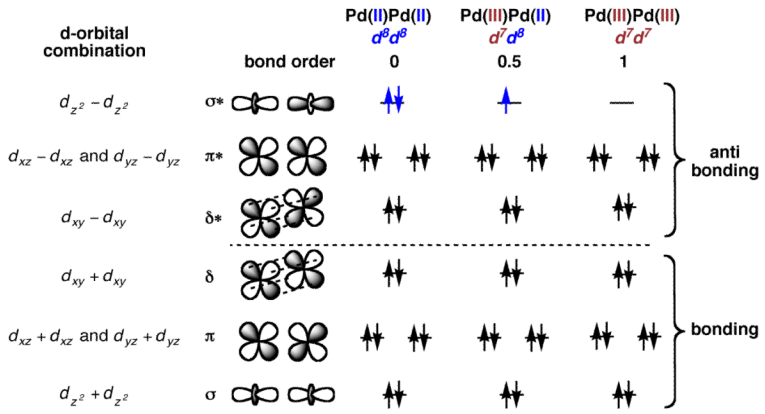

Fig. 20.

Qualitative molecular orbital diagram for electronically coupled dinuclear Pd complexes based on d-orbital mixing. Oxidation of dinuclear Pd(II) complexes can result in the formation of metal–metal bonds

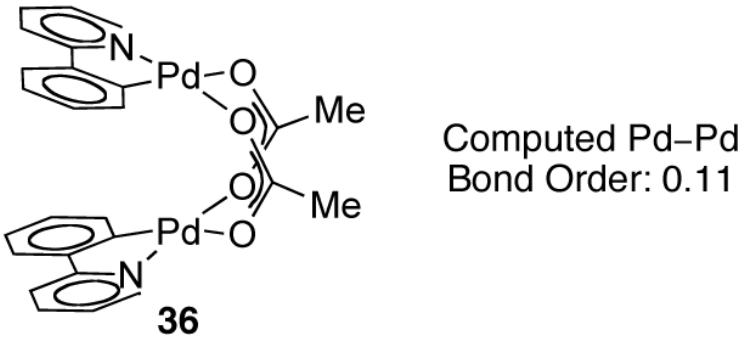

Fig. 21.

Acetate-bridged dinuclear Pd(II) complex **36** is computed to have a Pd–Pd bond order of 0.11, arising from mixing of the 5p_z and 5*s* orbitals with the 4*d* orbitals

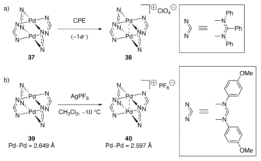

Fig. 22.

a) Electrochemical oxidation of **37** afforded mixed valence Pd(II)/Pd(III) complex **38**. b) One-electron oxidation of **39** with $AgPF_6$ afforded **40**. The Pd–Pd distance in **40** is consistent with a Pd–Pd bond order of 0.5

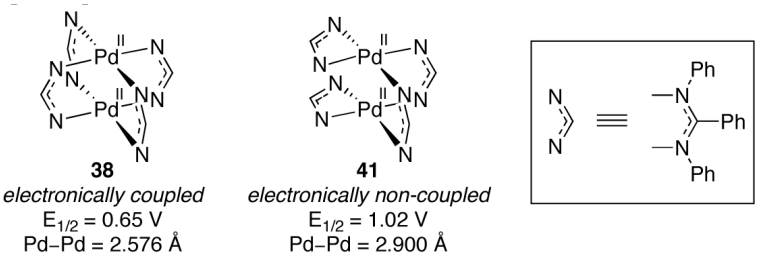

Fig. 23.

The HOMO of **38**, in which the Pd centers are electronically coupled, is 370 mV higher in energy than the HOMO of **41**, in which the palladium centers are not electronically coupled

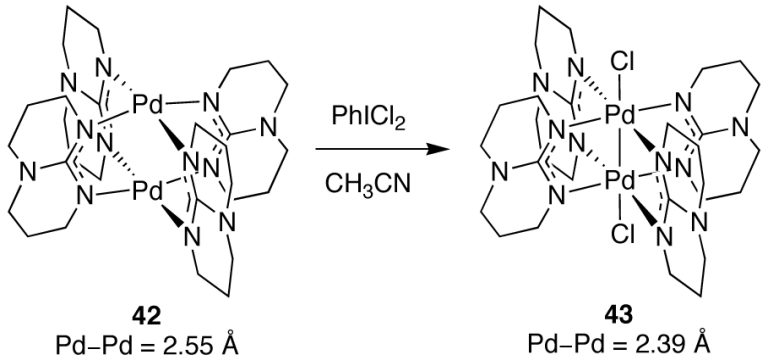

Fig. 24.
In 1998, Cotton reported the first dinuclear Pd(III) complex (**43**), obtained by oxidation of **42** with $PhICl_2$

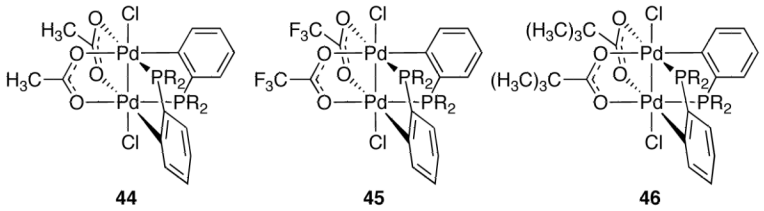

Fig. 25.
Early examples of organometallic dinuclear Pd(III) complexes (R = Ph)

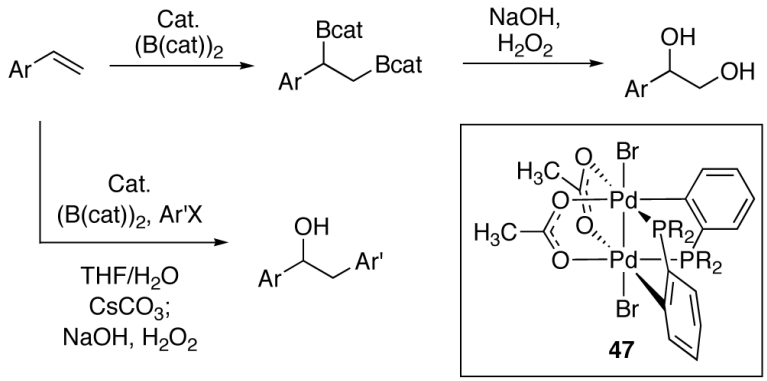

Fig. 26.

Dinuclear Pd(III) precatalysts in diborylation and borylation/cross-coupling tandem reactions (R = Ph; $(B(cat))_2$ = bis(pinacolato)diboron)

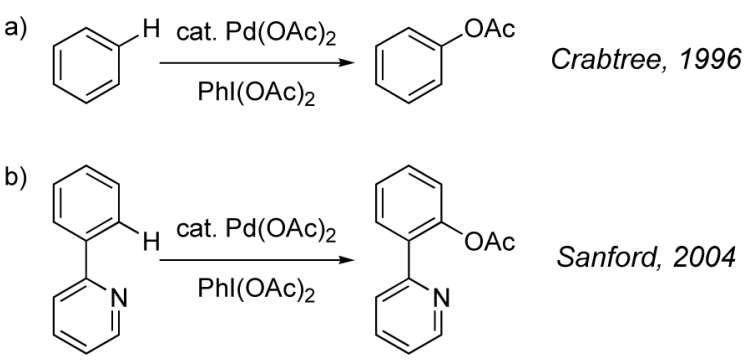

Fig. 27.
Pd-catalyzed aromatic C–H acetoxylation reactions with $PhI(OAc)_2$

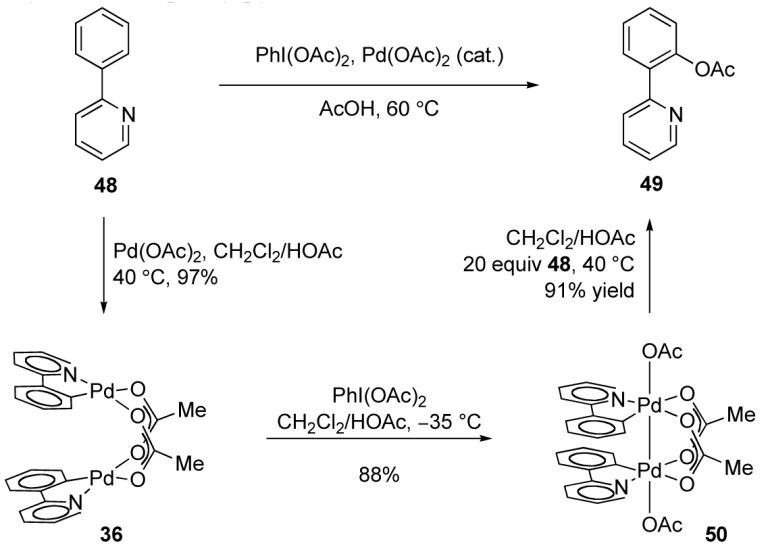

Fig. 28.

A synthesis cycle for the acetoxylation of 2-phenylpyridine (**48**) based on dinuclear Pd(III) complex **50** has been established

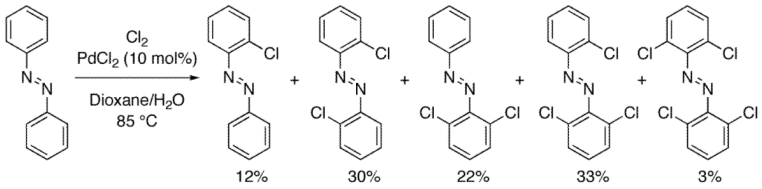

Fig. 29.
Chlorination of azobenzene reported by Fahey

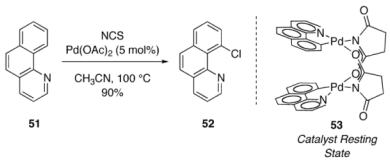

Fig. 30.

The resting state of Pd-catalyzed chlorination of benzo[*h*]quinoline (**51**) is succinate-bridged dinuclear Pd complex **53**. Pd–Pd bond length in **53**: 2.8628(4) Å

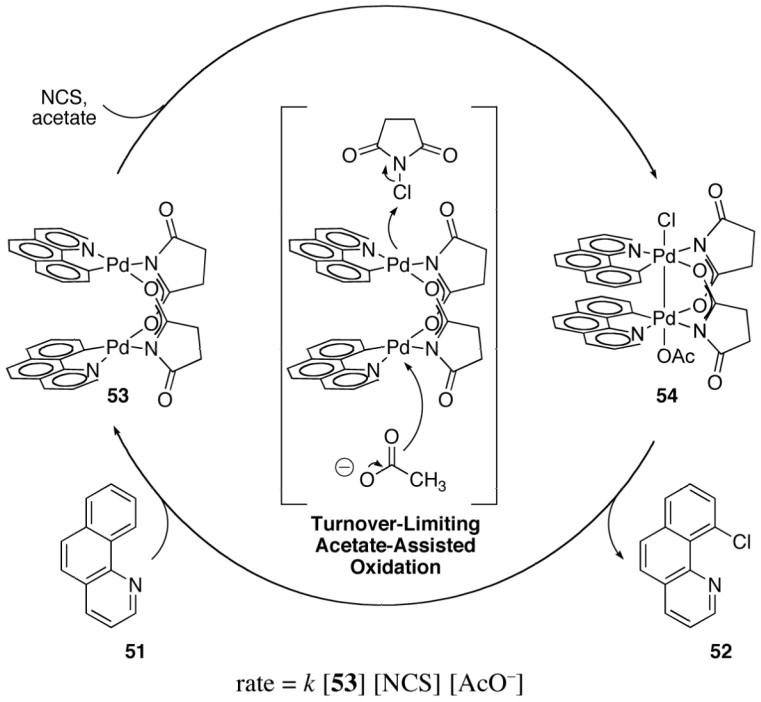

Fig. 31.

Proposed acetate-assisted bimetallic oxidation of **53** would afford dinuclear Pd(III) complex **54** immediately following oxidation

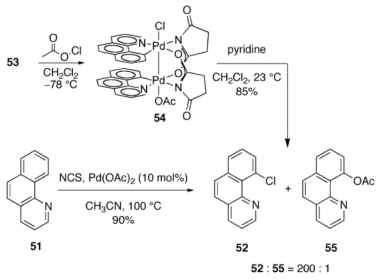

Fig. 32.

The ratio of **52** to **55** obtained by thermal decomposition of dinuclear Pd(III) complex **54** is similar to the ratio of **52** to **55** obtained by $Pd(OAc)_2$-catalyzed chlorination of benzo[*h*]quinoline (**51**) with NCS

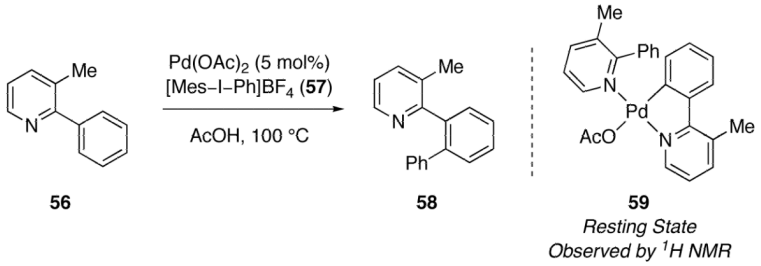

Fig. 33.

The catalyst resting state for the $Pd(OAc)_2$-catalyzed arylation of 3-methyl-2-phenylpyridine (**56**) is proposed to be mononuclear Pd(II) complex **59**

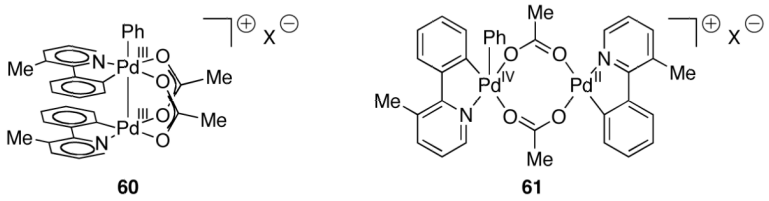

Fig. 34.

Formulations of the high-valent, dinuclear Pd complex proposed by Sanford in the arylation of 2-arylpyridine derivatives

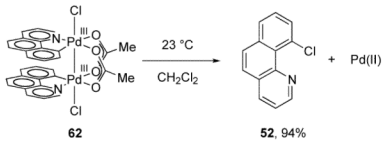

Fig. 35.
C–Cl reductive elimination from dinuclear Pd(III) complex **62**

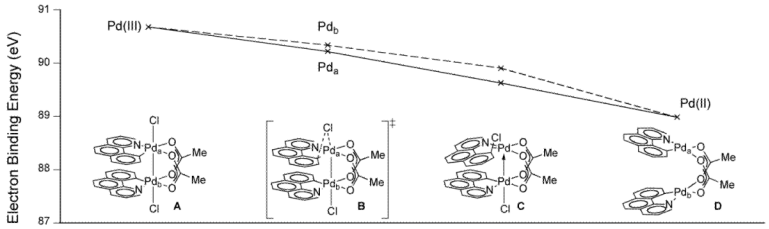

Fig. 36.

Electron binding energies as a function of reaction progress for C–Cl reductive elimination from dinuclear Pd(III) structure **A**

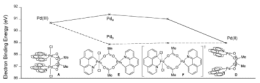

Fig. 37.
Electron binding energy as a function of reaction progress for monometallic reductive elimination via a Pd(II)/Pd(IV) mixed valence structure

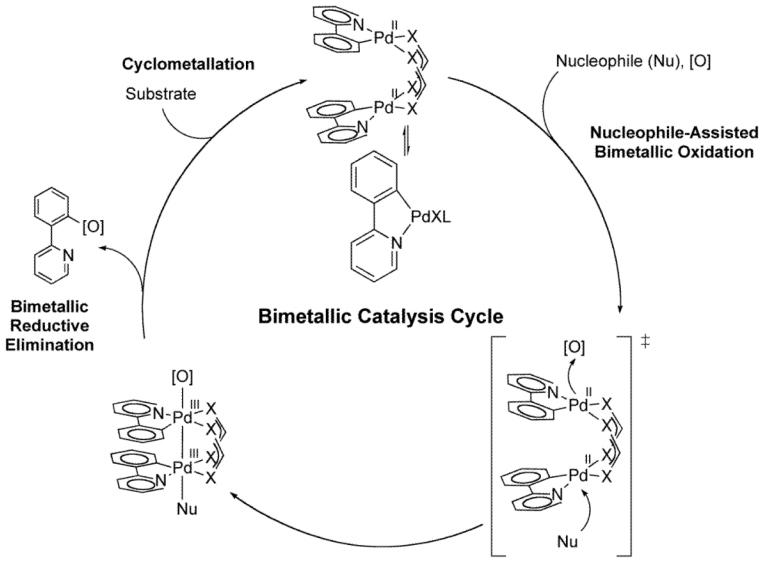

Fig. 38.
Proposed bimetallic $Pd(II)_2/Pd(III)_2$ catalysis cycle